BNL-52246
UC - 414 (High Energy Physics - DOE/OSTI-4500-R75)

Control of Non-Linear Space-Charge Emittance Growth

Juan C. Gallardo
Center for Accelerator Physics
Brookhaven National Laboratory
Upton, New York 11973

BNL--52246
DE90 014752

(Received)

A simple analytical model of the space-charge (self-fields) of a few picosecond electron pulse in a RF photocathode electron gun is presented. The model permits a search for the optimal laser distribution (transverse and longitudinal) that will result in an electron beam with minimum transverse emittance. It is concluded that electron distributions with sharp edges in the transverse dimension and parabolic (inverted) in the longitudinal direction are best to minimize the emittance. These effects have been confirmed with extensive simulations using the numerical code PARMELA.

INTRODUCTION

Single pass self amplified spontaneous emission (SASE) FELs require electron beams whose brightness is higher than what has been achieved so far. At the Accelerator Test Facility (ATF) we are studying the development of higher-brightness sources suitable to drive short wavelength FELs (XUV and X-ray). The gain length $L_G = \frac{\lambda_w}{4\pi\rho}$of the device is proportional to the brightness, $B_n^{-\frac{1}{3}}$ where $B_n \sim \frac{I}{\epsilon_n^2}$ and λ_w is the period of the wiggler; furthermore, the shortest coherent radiation achievable is determined by the emittance of the e^- beam, $\lambda \approx \frac{\epsilon_n}{\gamma}$. It is apparent that any reduction of the emittance will enhance the brightness and consequently decrease the gain length and simultaneously, we have potential access to shorter wavelength by either increasing the electron beam energy γ or decreasing the wiggler period λ_w.

The intrinsic (thermal) normalized emittance of the cathode is given by $\epsilon_n = \frac{1}{2} r_c \sqrt{\frac{kT}{mc^2}}$ which corresponds to an intrinsic normalized brightness

$$B_n = \frac{4}{\pi} J_c \frac{mc^2}{kT} \tag{1}$$

where we have used $I = J_c \pi r_c^2$; for $J_c \approx 600 \frac{\mathrm{A}}{\mathrm{cm}^2}$ and $kT = 1eV$, $B_n = 3.9 \times 10^{12} \frac{A}{(m-rad)^2}$. There are several other factors that significantly reduce the actual brightness of our gun with respect to the cathode brightness. The more important are time dependent forces introduced by the RF field and space charge forces, both of which are non-linear and *time* dependent (i.e., function of the position in the beam). This reduction of B_n is due to emittance growth, i.e. higher order correlations in phase-space xx'. This is the result of the variation of the space charge forces along the length of the pulse. This dependence produces that the ellipse in phase space, representing a section of the beam, changes orientation as we consider consecutive sections; this is the origin of the well known fan figure in phase space (Fig. 1). The area associated with each section could be small but the emittance of the entire beam is a figure of merit of the composite of all ellipses and, consequently, is larger than the individual ones. We turn now to a discussion of a possible way of controlling the *time* dependence of space-charge forces within the context of a simple analytical model of the e^- beam close to the cathode.

SIMPLE ANALYTICAL MODEL

Let us consider a laser pulse of $\tau_L = 6\,\mathrm{ps}$ and transverse radius $\sim 2-3\,\mathrm{mm}$. We assume that an identical e^- beam is created with initial energy $T \approx 0.5\,\mathrm{eV}$. We divide the beam along the longitudinal axis into a collection of disks of radius $r = a$ and we calculate the self-fields (space charge fields) created by each disk. We then add all the individual disks' fields to obtain the total space charge force acting on each electron.

The functional form of the radial component of the electric field $E_r(r,z)$ (in the rest frame of the beam), as a function of r and z, will reflect itself in the radial momentum of the electrons $p_r = \frac{e}{c}\int \frac{dz}{\beta_z\gamma} E_r(r,z)$ and, consequently in the transverse emittance, substituting in the emittance definition $\epsilon_\perp = \sqrt{<p_r^2><r^2> - <rp_r>^2}$ we obtain[1] $\epsilon_\perp \propto \sqrt{<E_r^2><r^2> - <rE_r>^2}$. First we solve for the potential function $V(r,z)$ created by a single disk of radius a and surface charge density σ. We solve the Laplace equation $\Delta V(r,z) = 0$ with the boundary conditions

$$\frac{\partial V}{\partial z}|_{z=0} = -2\pi\sigma \qquad 0 \le r \le a \tag{2}$$

$$\frac{\partial V}{\partial z}|_{z=0} = \quad 0 \qquad\qquad r \le a \tag{3}$$

Assuming $V(r,z) = f(r)g(z)$ and after some simple manipulations, the Laplace equation reads,

$$\frac{1}{f}\left\{f'' + \frac{1}{r}f'\right\} = -\frac{g''}{g} = -\alpha^2 \tag{4}$$

where α is a constant. We then write, $g(z) = e^{-\alpha|z|}$ and $f(r) = J_0(\alpha r)$; hence,

$$V(r,z) = \int_0^\infty dx J_0(x\frac{r}{a})A(x)e^{-x\frac{|z|}{a}} \qquad (5)$$

where we have defined $\alpha = \frac{z}{a}$. Using the Bessel integral

$$\int_0^\infty dx J_0(x\frac{r}{a})J_1(x) = \begin{cases} 1 & 0 \le \frac{r}{a} \le 1 \\ 0 & \text{otherwise.} \end{cases} \qquad (6)$$

and the boundary conditions, we obtain $A(x) = 2\pi\sigma\frac{a}{x}J_1(x)$ if σ = constant; consequently, the potential functions is

$$V(r,z) = 2\pi\sigma a \int_0^\infty dx J_0(x\frac{r}{a})\frac{J_1(x)}{x}e^{-x\frac{|z|}{a}} \qquad (7)$$

On the other hand, if $\sigma(r/a) = \sigma_0(1-(r/a)^2)$, then $A(x) = 8\pi\sigma_0\frac{a}{x^2}J_2(x)$ and the potential function is

$$V(r,z) = 8\pi\sigma a \int_0^\infty dx J_0(x\frac{r}{a})\frac{J_2(x)}{x^2}e^{-x\frac{|z|}{a}}. \qquad (8)$$

Adding the contribution of all the disks we can calculate the electric field $\vec{E}(r,z) = -\vec{\nabla}V(r,z)$ at any point (r,z). Care must be taken with the position of the disk and the absolute value in the exponential. We also add the contribution of the image charge due to the metallic surface of the cathode. Next, we generalize the result to an arbitrary longitudinal distribution of surface charge density $\sigma(z)$. Our working expression for the electric field are,

$$\begin{aligned} E_r(r,z) = {} & \tfrac{2\pi}{L}\int_0^\infty dx J_1(x\tfrac{r}{a})B_m J_m(x)\Big\{\int_0^z dz'\sigma(z')e^{-\frac{x}{a}(z-z')} \\ & + \int_z^L dz'\sigma(z')e^{\frac{x}{a}(z-z')} - \int_0^L dz'\sigma(z')e^{-\frac{x}{a}(z+z'+z_b)}\Big\} \qquad (9) \\ E_z(r,z) = {} & \tfrac{2\pi}{L}\int_0^\infty dx J_0(x\tfrac{r}{a})B_m J_m(x)\Big\{\int_0^z dz'\sigma(z')e^{-\frac{x}{a}(z-z')} \\ & - \int_z^L dz'\sigma(z')e^{\frac{x}{a}(z-z')} - \int_0^L dz'\sigma(z')e^{-\frac{x}{a}(z+z'+z_b)}\Big\} \qquad (10) \end{aligned}$$

where r is the radial coordinate, z is the relative coordinate respect to the back of the pulse and z_b is its actual position respect to the cathode; we have also defined

$$B_m J_m = \begin{cases} J_1(x) \quad \text{for } \sigma = \sigma_0 \\ \frac{4}{x} J_2(x) \, \text{for } \sigma = \sigma_0(1 - (r/a)^2). \end{cases} \tag{11}$$

Figs. 2 and 3 show the radial and longitudinal electric field for an electron beam with rectangular transverse and inverted parabolic longitudinal distributions. We observe that E_r is nearly constant as a function of z and essentially linear with r. For comparison we present in Figs. 4 and 5 the self-fields for a parabolic transverse and *flat-top* longitudinal distributions; they show a curvature in $E_r(r, z)$ .vs. z and different slopes of $E_r(r, z)$ .vs. r which will result in a significant fan-like figure in phase space and consequently, a larger emittance than in the previous case.

CONCLUSIONS

To completely cancel the aberrations introduced by space-charge field, E_r must be linear in r and independent of z. This is best obtained using transverse distributions with sharp edges which tend to reduce the time dependence of the radial electric field and therefore, the emittance growth. Furthermore, to compensate for the decrease of the space charge at both ends of the pulse, an inverted parabolic longitudinal distribution will tend to further reduce the extend of the fan in phase space.

The results of this simple analytical model of the space-charge forces have been confirmed with extensive simulation[2] (see, Table 1) using the code PARMELA[3].

An experimental test of these ideas will be performed with the RF photocathode gun at the Accelerator Test Facility, Brookhaven National Laboratory.

ACKNOWLEDGEMENT

This work was supported by the U.S. Department of Energy under Contract No. DE-AC02-76-CH00016. I would like to thanks R. Palmer for his support and valuable discussions and also to I. Ben-Zvi for helpful conversations.

[1] K.-J. Kim, *RF and Space-Charge Effects in Laser-Driven RF Electron Guns*, **LBL-25807**, (1988).

[2] Juan Gallardo and Robert Palmer, *Preliminary study of gun emittance corrections*, IEEE J. Quantum Electron., **xxx**, August (1990).

[3] K. Crandall and L. Young, private communication.

FIG. 1. Phase space plot showing a typical fan-like shape

FIG. 2. Radial self-field for an electron beam of 3 mm radius and 6 ps length. Rectangular transverse and parabolic (inverted) longitudinal distribution. a) $E_r(r,z)$ .vs. z showing no z dependence for $r \leq$ 2mm; b) $E_r(r,z)$ .vs. r showing a constant linear dependence with r.

FIG. 3. Longitudinal self-field for the same electron beam of Fig 2. a) $E_z(r,z)$ .vs. z ; b) $E_z(r,z)$ .vs. r

FIG. 4. Radial self-field for an electron beam of 3 mm radius and 6 ps length. Parabolic transverse and *flat-top* longitudinal distribution. a) $E_r(r,z)$ .vs. z showing a z dependence; b) $E_r(r,z)$ .vs. r showing changing slopes as we move along the beam axis.

FIG. 5. Longitudinal self-field for the same electron beam of Fig 4. a) $E_z(r,z)$ .vs. z ; b) $E_z(r,z)$ .vs. r

TABLE I. Results of simulations using the code PARMELA for different initial electron distributions.

cathode radius r [mm]	3
pulse length τ [ps]	6
charge Q [nC]	1

Normalized Emittance $\epsilon_n [mm - mrad]$	
transverse gaussian	10.8
transverse rectangular	6.57
transverse rectangular, parabolic longitudinal	4.42

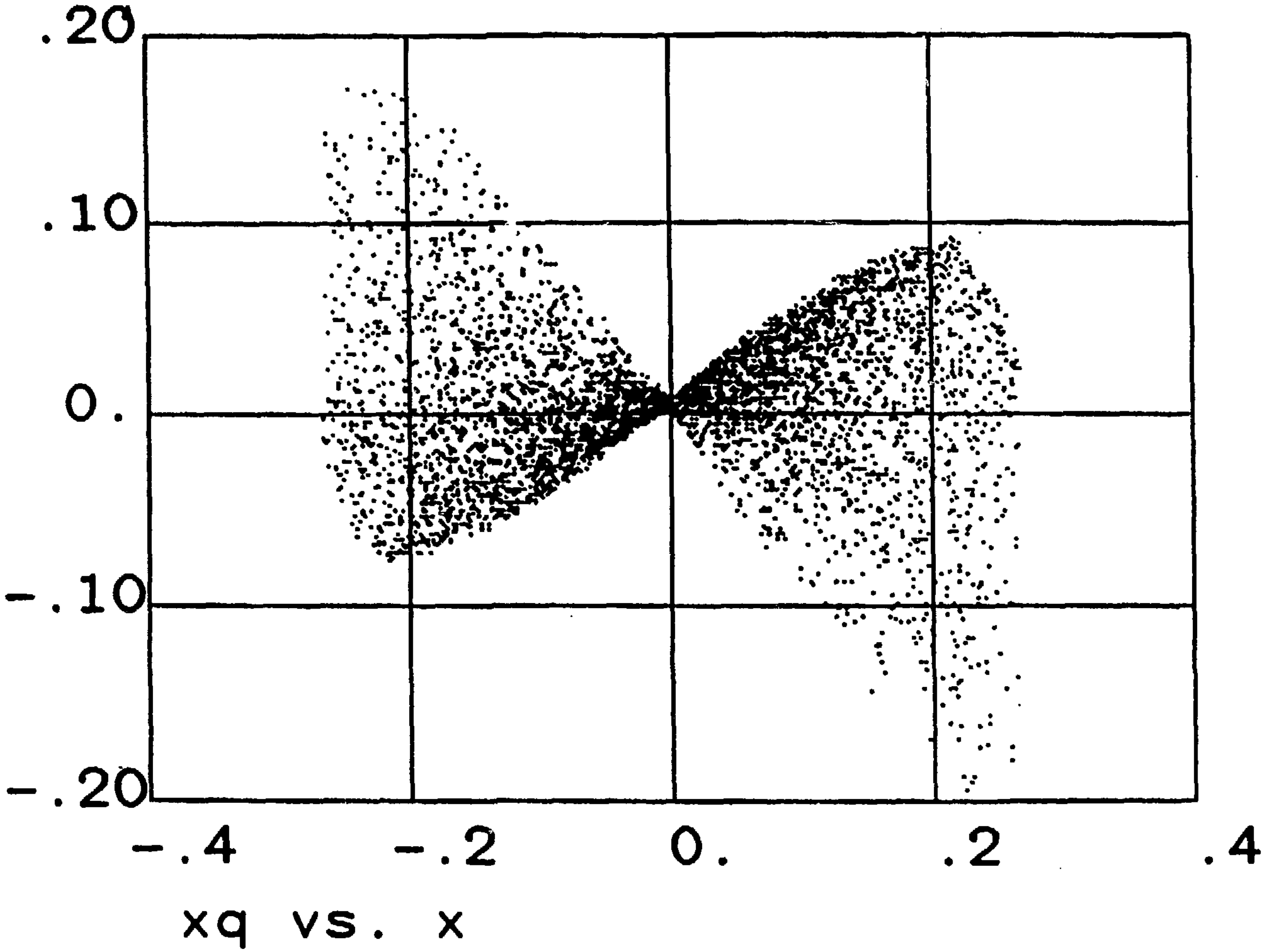

Fig. 1

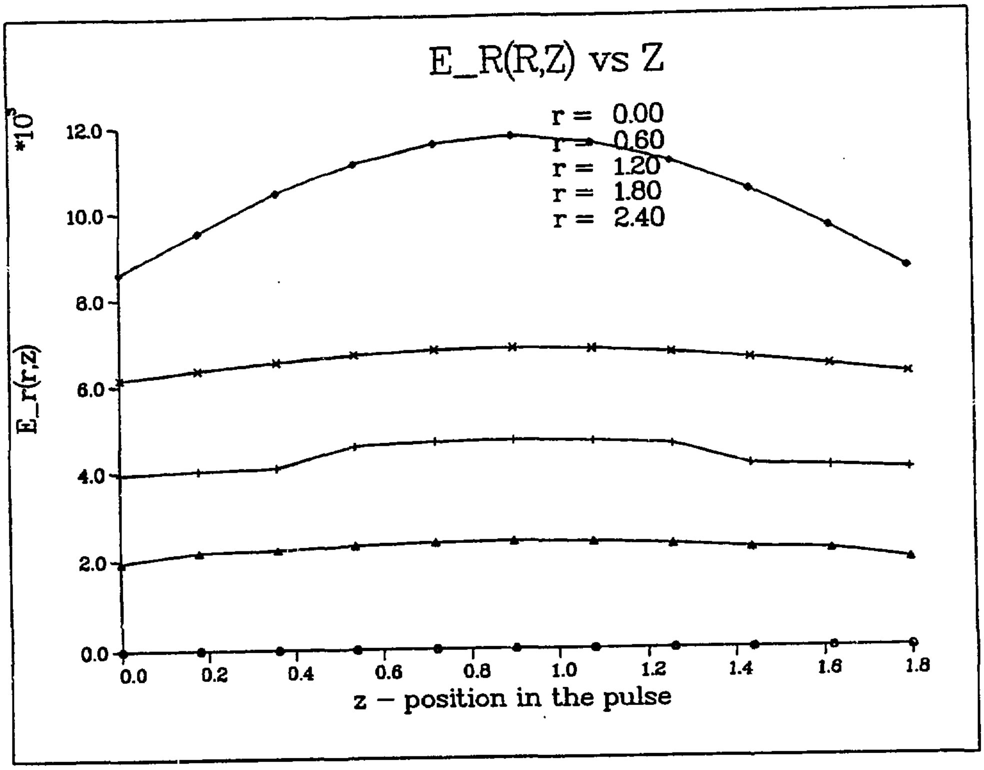
E_R(R,Z) vs Z
r = 0.00
r = 0.60
r = 1.20
r = 1.80
r = 2.40
*10^3
E_r(r,z)
z – position in the pulse

Fig. 2a

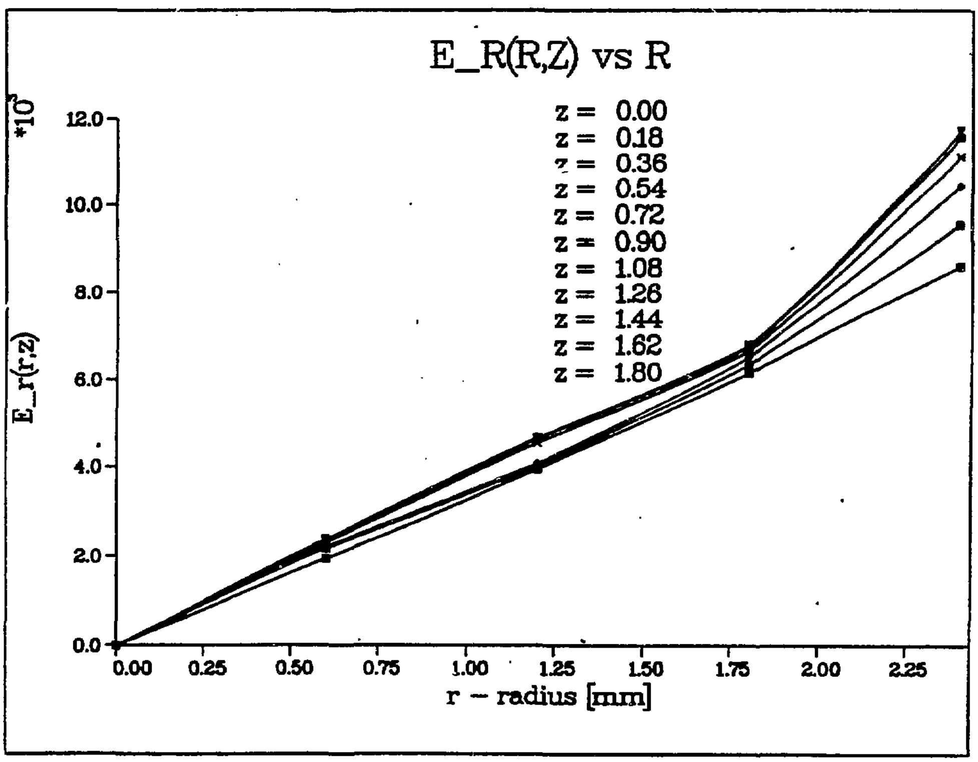
E_R(R,Z) vs R
z = 0.00
z = 0.18
z = 0.36
z = 0.54
z = 0.72
z = 0.90
z = 1.08
z = 1.26
z = 1.44
z = 1.62
z = 1.80
*10^3
E_r(r,z)
r – radius [mm]

Fig. 2b

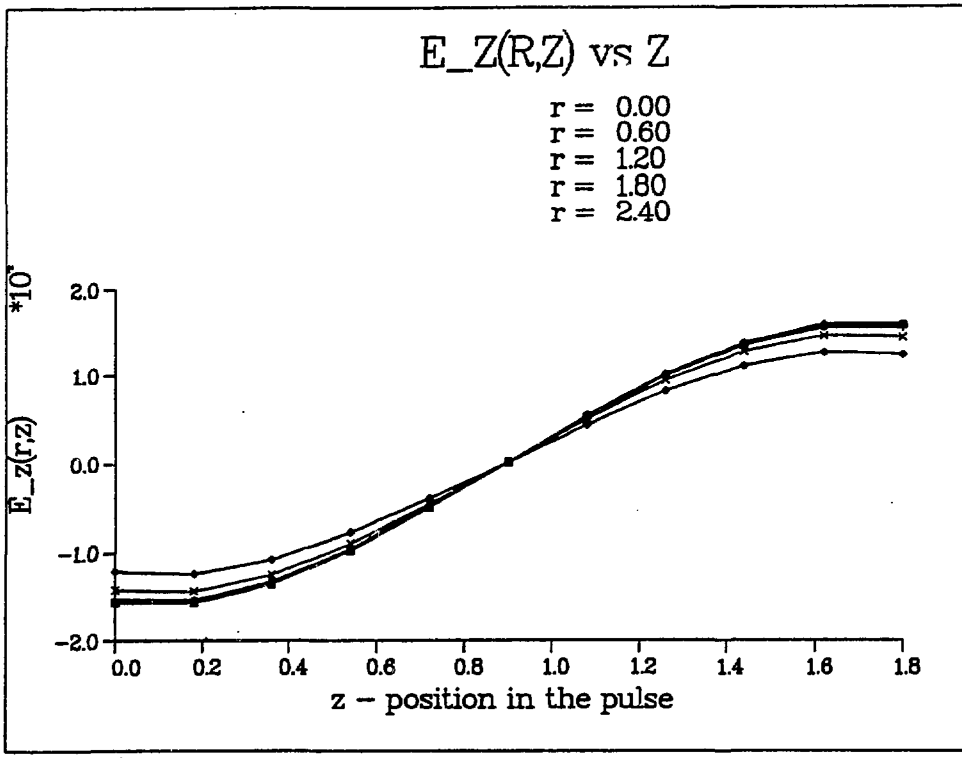

E_Z(R,Z) vs Z
r = 0.00
r = 0.60
r = 1.20
r = 1.80
r = 2.40
*10
E_z(r,z)
2.0
1.0
0.0
−1.0
−2.0
0.0
0.2
0.4
0.6
0.8
1.0
1.2
1.4
1.6
1.8
z − position in the pulse

Fig. 3a

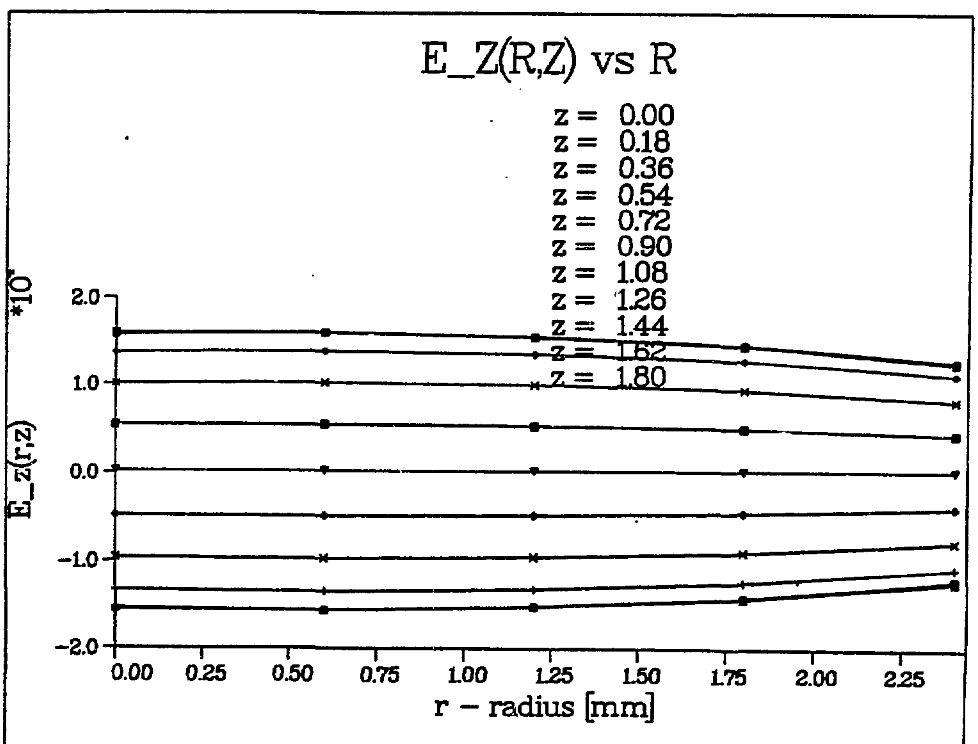

E_Z(R,Z) vs R
z = 0.00
z = 0.18
z = 0.36
z = 0.54
z = 0.72
z = 0.90
z = 1.08
z = 1.26
z = 1.44
z = 1.62
z = 1.80
*10
E_z(r,z)
2.0
1.0
0.0
−1.0
−2.0
0.00
0.25
0.50
0.75
1.00
1.25
1.50
1.75
2.00
2.25
r − radius [mm]

Fig. 3b

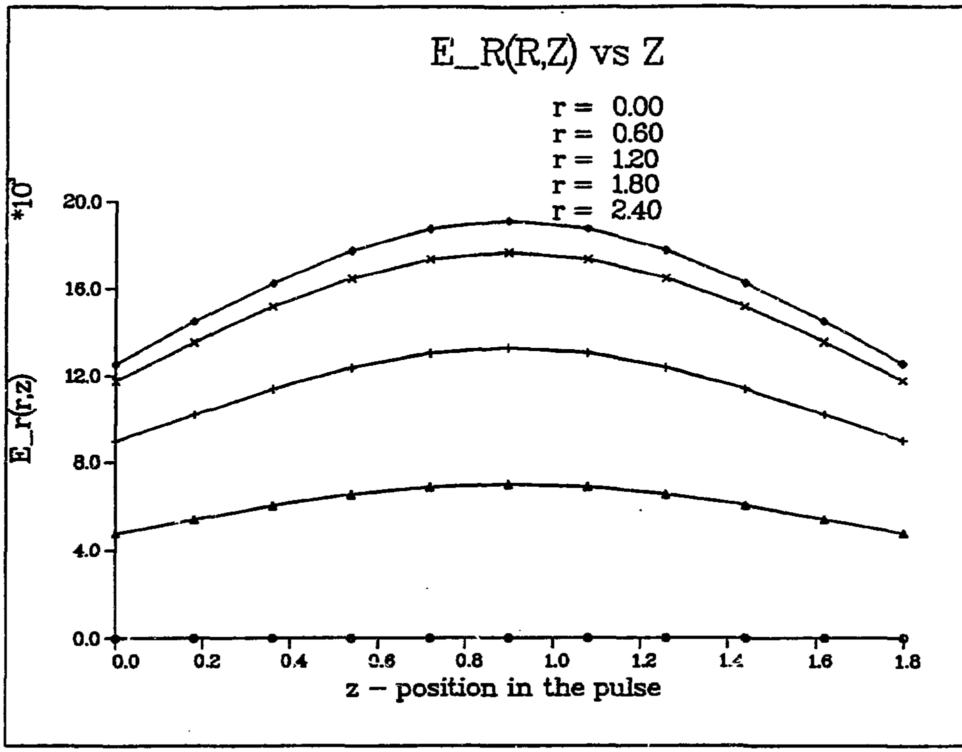
E_R(R,Z) vs Z
r = 0.00
r = 0.60
r = 1.20
r = 1.80
r = 2.40
*10
E_r(r,z)
20.0
16.0
12.0
8.0
4.0
0.0
0.0
0.2
0.4
0.6
0.8
1.0
1.2
1.4
1.6
1.8
z – position in the pulse

Fig. 4a

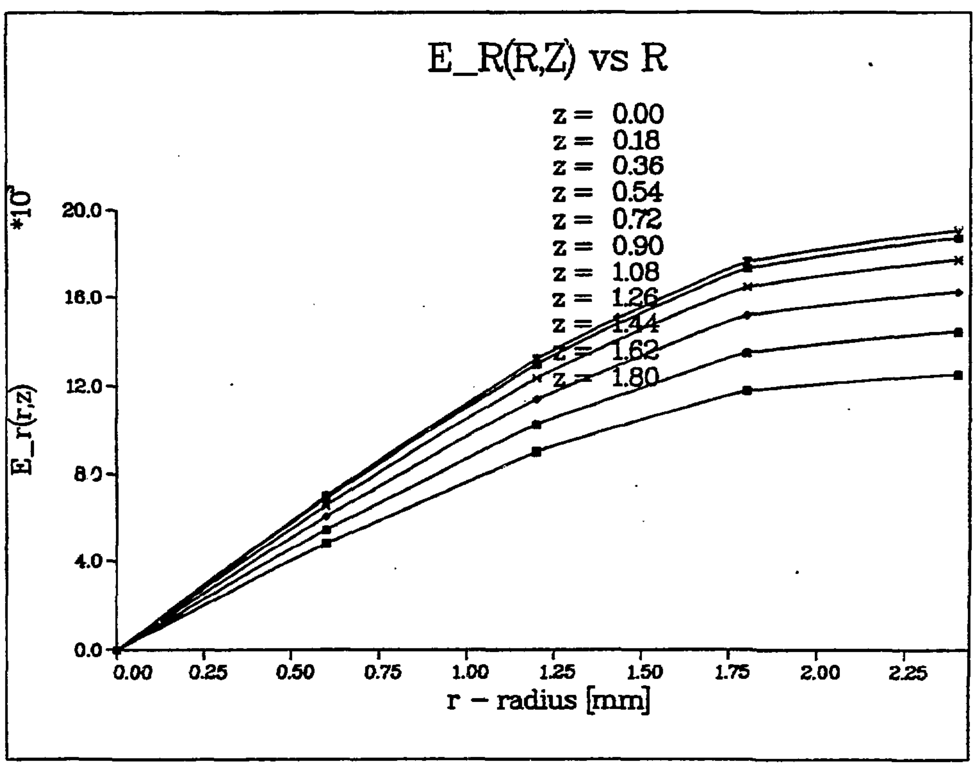
E_R(R,Z) vs R
z = 0.00
z = 0.18
z = 0.36
z = 0.54
z = 0.72
z = 0.90
z = 1.08
z = 1.26
z = 1.44
z = 1.62
z = 1.80
*10
E_r(r,z)
20.0
16.0
12.0
8.0
4.0
0.0
0.00
0.25
0.50
0.75
1.00
1.25
1.50
1.75
2.00
2.25
r – radius [mm]

Fig. 4b

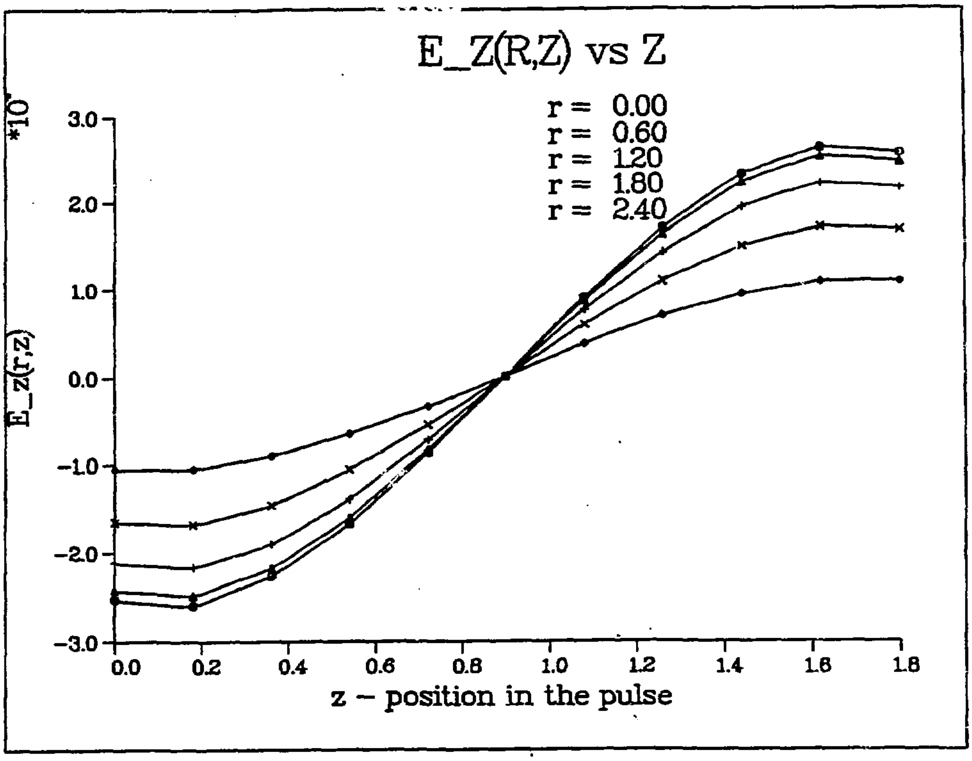
E_Z(R,Z) vs Z
*10
r = 0.00
r = 0.60
r = 1.20
r = 1.80
r = 2.40
3.0
2.0
1.0
0.0
−1.0
−2.0
−3.0
E_z(r,z)
0.0
0.2
0.4
0.6
0.8
1.0
1.2
1.4
1.6
1.8
z − position in the pulse

Fig. 5a

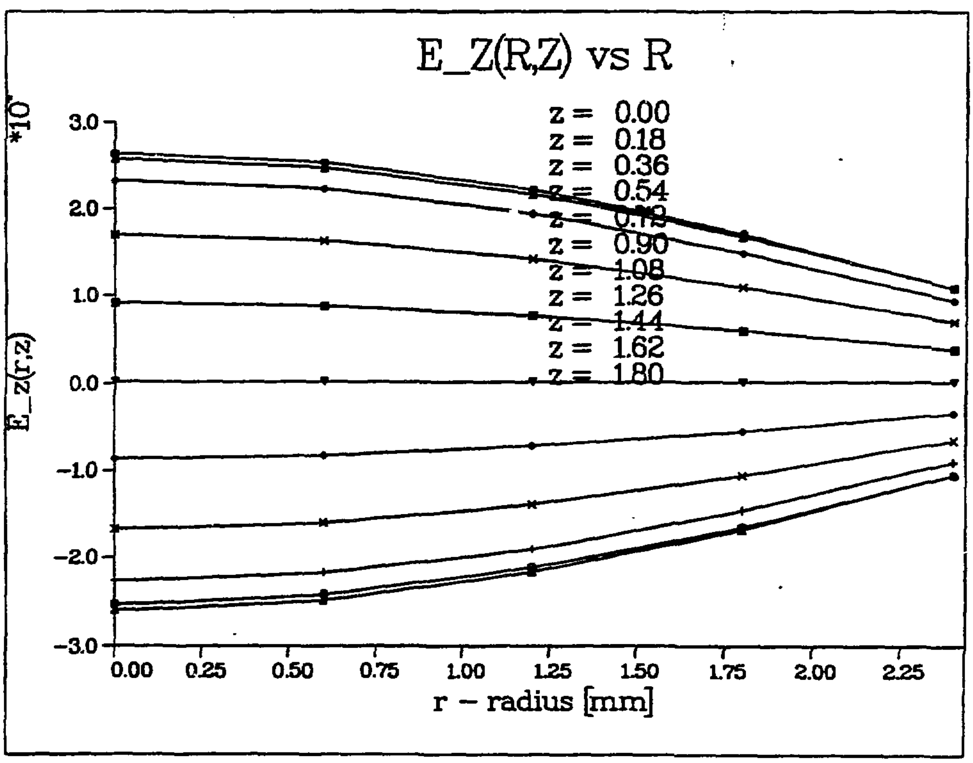
E_Z(R,Z) vs R
*10
z = 0.00
z = 0.18
z = 0.36
z = 0.54
z = 0.72
z = 0.90
z = 1.08
z = 1.26
z = 1.44
z = 1.62
z = 1.80
3.0
2.0
1.0
0.0
−1.0
−2.0
−3.0
E_z(r,z)
0.00
0.25
0.50
0.75
1.00
1.25
1.50
1.75
2.00
2.25
r − radius [mm]

Fig. 5b